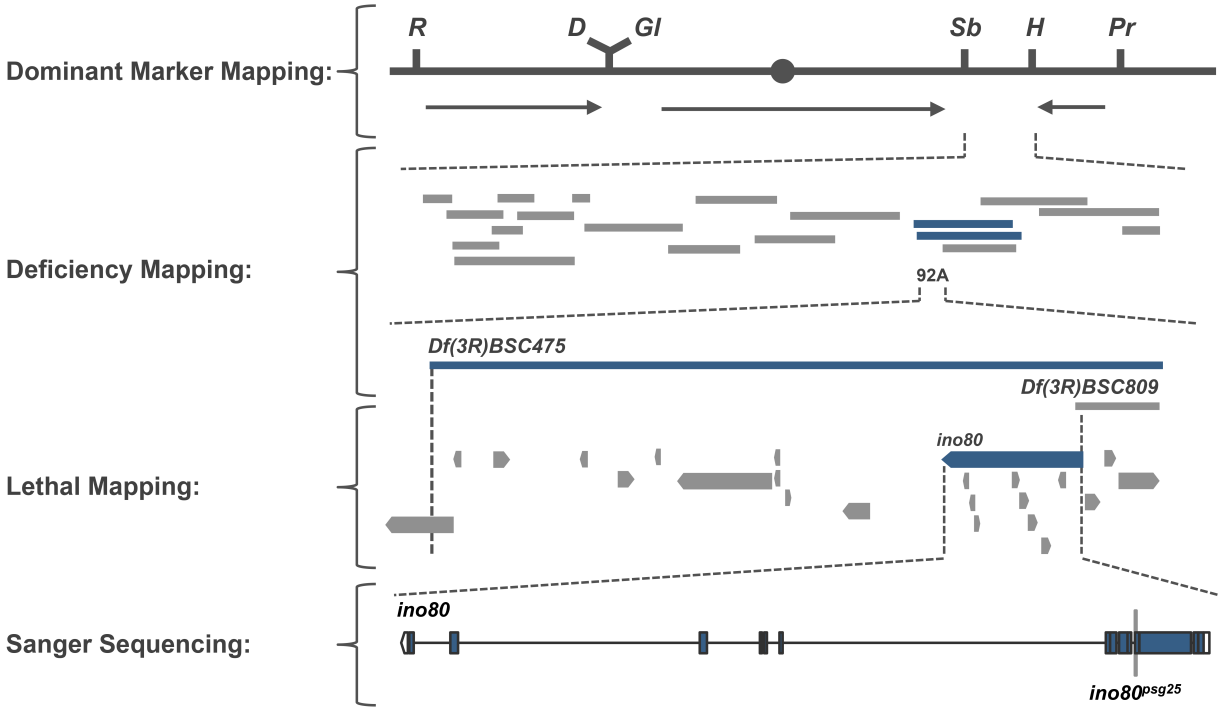

Figure S1. Mapping of the *psg25* mutation. *psg25* was mapped by dominant marker recombination, complementation tests, and Sanger sequencing. Recombination mapping with pairs of dominant markers placed *psg25* in the *Stubble* (*Sb*), *Hairless* (*H*) region, right of the *Roughened* (*R*), *Dichaete* (*D*) and *Glued* (*Gl*), *Stubble* (*Sb*) regions and left of the *Hairless* (*H*), *Prickly* (*Pr*) region (see arrows, method described in Sapiro *et al.* 2013). *psg25* failed to complement two overlapping chromosomal deficiencies, but complemented all available lethals in the region. Sanger sequencing of candidate genes identified a lesion disrupting the donor splice site after the fourth exon of *ino80*. The entire *ino80* locus encompasses over 34 kilobases.

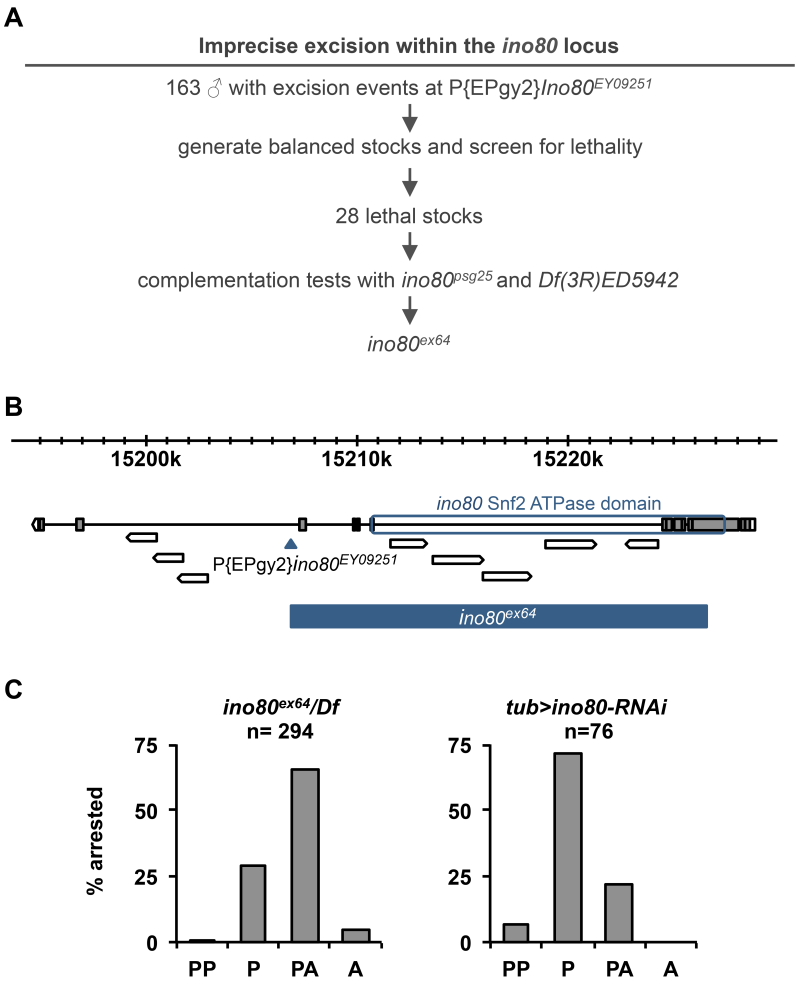

Figure S2. Generation of a second *ino80* allele via imprecise excision. **(A)** Diagram of crosses used to generate imprecise excision stocks. Of 163 excision events tested, only one excision, *ex64*, failed to complement the *ino80*-containing chromosomal deficiency. **(B)** Characterization of the molecular lesion in *ino80*^{ex64}. PCR analysis identified a large deletion within the *ino80* locus, removing most of the Snf2 ATPase domain and leaving a region of P-element sequence behind. **(C)** Lethal phase analysis of *ino80*^{ex64}*/Df* and ubiquitous expression of *ino80-RNAi* (*UAS-ino80-RNAi/UAS-Dcr-2; tubulin-GAL4*). Most *ino80*^{ex64} and *ino80-RNAi* animals arrest after head eversion, as pupae or pharate adults.

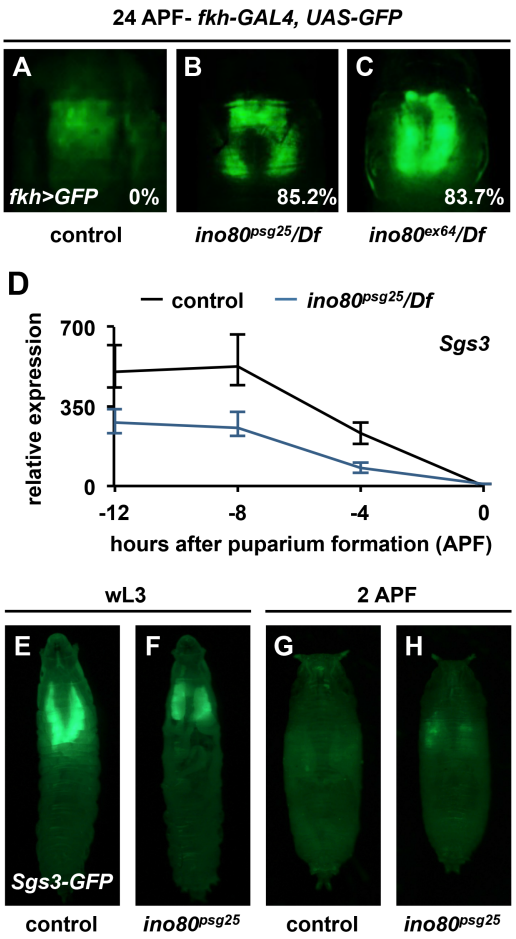

Figure S3. Analysis of ecdysone-dependent responses in *ino80*^{psg25} mutant salivary glands.
(A-C) *fkh-GAL4, UAS-GFP* expression in control (A), *ino80*^{psg25}*/Df* (B), and *ino80*^{ex64}*/Df* (C) mutant animals at 24 h after puparium formation (APF). (A) Control glands have diffuse GFP expression, indicating the glands have been eliminated via programmed cell death. (B-C) *ino80*^{psg25} and *ino80*^{ex64} mutant animals have strong expression of GFP at 24 APF, indicative a persistent salivary gland phenotype (85.2%, n=54 and 83.7%, n=37, respectively). **(D)** qPCR analysis of *Sgs3* mRNA expression in control (black line) and *ino80*^{psg25} (blue line) mutant whole animals. *Sgs3* transcription is induced and repressed properly in *ino80*^{psg25}. *y*-axis represents relative expression compared to the lowest point in control animals; *x*-axis represents developmental stage relative to puparium formation (APF). Three independently-isolated samples were run for each timepoint; relative expression calculated by normalizing to *rp49*. **(E-H)** Sgs3-GFP expression in control (E,G) and *ino80*^{psg25} (F,H) mutant animals. (E,F) Both genotypes robustly express Sgs3-GFP in wL3, indicating that *ino80*^{psg25} does not disrupt glue protein synthesis. (G,H) Sgs3-GFP is no longer present in salivary glands of either genotype at 2 APF, indicating that *ino80*^{psg25} does not disrupt glue protein secretion.

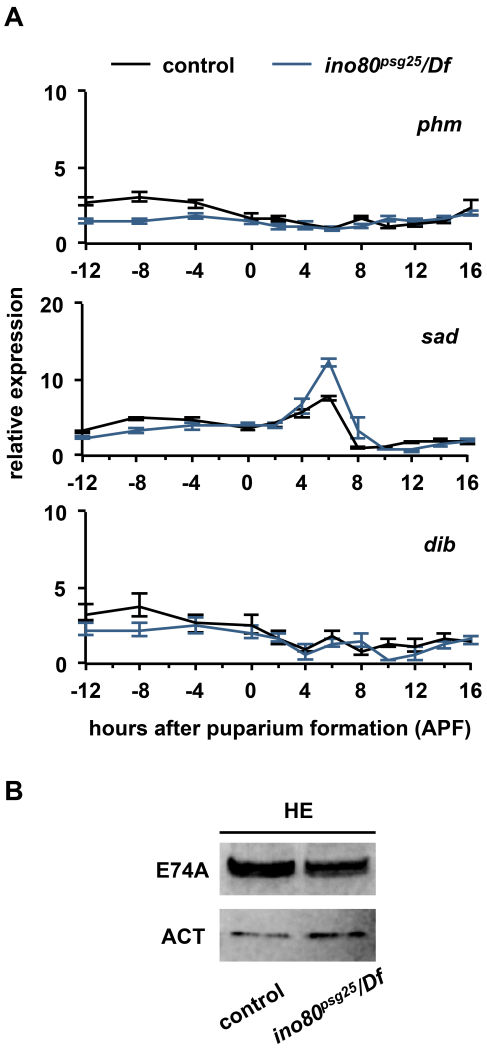

Figure S4. *ino80* is not required for repression of all genes during prepupal development.
(A) qPCR analysis of ecdysone biosynthesis genes in whole animals staged relative to puparium formation. *ino80*^{psg25} (blue line) does not disrupt expression of *phantom (phm)*, *shadow* (*sad*), or *disembodied* (*dib*) when compared to controls (black line). *y*-axis represents relative expression compared to the lowest point in control animals; *x*-axis represents developmental stage relative to puparium formation (APF). Three independently-isolated samples were run for each timepoint; relative expression calculated by normalizing to *rp49*. **(B)** Western blot for E74A protein in control and *ino80*^{psg25} mutant whole animals at head eversion. E74A is robustly translated in both control and *ino80*^{psg25} animals. β-actin used as a loading control.

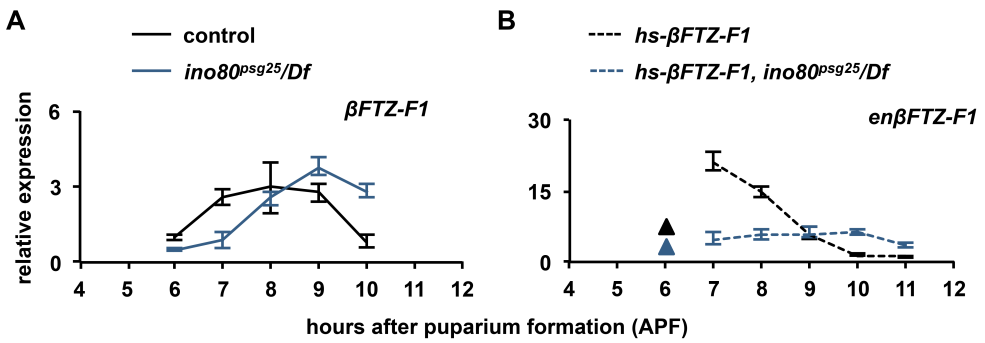

Figure S5. Regulation of *βFTZ-F1* expression in control and *ino80*^{psg25} mutant animals. (A) qPCR analysis of *βFTZ-F1* expression in control (black line) and *ino80*^{psg25} mutant (blue line) animals in one-hour increments. *βFTZ-F1* induction is delayed by about 1 hour in *ino80*^{psg25}. *y*-axis plots relative expression compared to the lowest point in controls; *x*-axis represents hours relative to puparium formation. Three independently-isolated whole animal samples were run for each timepoint and normalized to *rp49*. **(B)** Expression of βFTZ-F1 protein at 6 APF abolishes endogenous *βFTZ-F1* transcription in *ino80*^{psg25} mutant animals. qPCR analysis of endogenous *βFTZ-F1* expression after heat-treatment with *hs-βFTZ-F1* at 6 APF in control (dashed black line) and *ino80*^{psg25} mutant (dashed blue line) animals. *y*-axis plots relative expression compared to the lowest point in controls; *x*-axis represents stages relative to puparium formation. Three independently-isolated whole animal samples were run for each timepoint and normalized to *rp49*. Triangles denote the time of heat-shock (black=control, blue=*ino80*^{psg25}).

TABLE S1. Primer sequences for qPCR

Gene	Primer Sequence	Source
Cyp18a1 F	TCTTCGATGGCAAGAATCACGAG	This Study
Cyp18a1 R	TATCCACAGCAGGGTGGTCTTG	
DHR3 F	GGCAGGAGCTGGAAACGAATC	This Study
DHR3 R	GGTCCTGCTGCGAATCTATCG	
dib F	GTGACCAAGGAGTTCATTAGATTTC	(Deng and Kerppola, 2013)
dib R	CCAAAGGTAAGCAAACAGGTTAAT	
E74A F	GTTGCCGGAACATTATGGATATA	(Caldwell et al., 2005)
E74A R	GCCCTATGTCGGCTTGCT	
E74B F	ATCGGCGGCCTACAAGAAG	(Caldwell et al., 2005)
E74B R	TCGATTGCTTGACAATAGGAATTTC	
FTZ-F1 F	TGGACTACACCCTCACCTGC	(Ihry et al., 2012)
FTZ-F1 R	CACGTTCTCCCGGCCTCTAT	
enβFTZ-F1 F	TGCATGCACCGAATACAATA	This Study
enβFTZ-F1 R	GCTGTTCTGCTGGTGTGG	
hid F	ATCCAGTCTGCCATACCGATAG	(Ihry et al., 2012)
hid R	AACAGTTGGCCAAGTGAAGCTC	
ino80 F	GTTAAGGTGACGACGCTGCTG	This Study
ino80 R	CCTGGCTATTCTCACACTGATTG	
phm F	TTTCGGCGCGATGTGATGACTG	This Study
phm R	GCGCAGATGATGCCAAATCCAC	
rp49 F	CCAGTCGGATCGATATGCTAA	(Denton et al., 2009)
rp49 R	ACGTTGTGCACCAGGAACTT	
rpr F	ATCCGAAGACCGGAAGAAAG	(Ihry et al., 2012)
rpr R	GTGGCTCTGTGTCCTTGACTG	
sad F	GATGTGCCAGGCGATATGAT	(Deng and Kerppola, 2013)
sad R	ACTGCTGAATGCGGTCGT	
Sgs3 F	CTACCGCCCTAGCGAGCAT	(Chiang and Kurnit, 2003)
Sgs3 R	GCATCCACAATCGCAACAGT	
spok F	GCGGTGATCGAAACAACTC	(Deng and Kerppola, 2013)
spok R	CGAGCTAAATTTCTCCGCTTT	